

# Adsorption, Desorption, and Conversion of Thiophene on H-ZSM5

Antonio Chica,<sup>†</sup> Karl Strohmaier,<sup>‡</sup> and Enrique Iglesia<sup>\*,†</sup>

Department of Chemical Engineering, University of California at Berkeley, Berkeley, California 94720, and ExxonMobil Research and Engineering, Corporate Strategic Research Labs, Annandale, New Jersey 08801

Received July 6, 2004. In Final Form: September 11, 2004

The dynamics and stoichiometry of thiophene adsorption and of rearrangements of thiophene-derived adsorbed species in O<sub>2</sub>, He, H<sub>2</sub>, and C<sub>3</sub>H<sub>8</sub> carriers were measured using chromatographic methods and mass spectrometry on H-ZSM5 and H-Y zeolites. Thiophene adsorption obeyed Langmuir isotherms on both zeolites. Adsorption uptakes were 1.7 and 2.8 thiophene/Al at 363 K on H-ZSM5 and H-Y zeolites, respectively, after removal of physisorbed thiophene. These stoichiometries differed for these two zeolite structures but did not depend on their Al content (Si/Al = 13–85). Adsorption from a thiophene–toluene mixture showed thiophene selectivities (~10) greater than expected from van der Waals interactions. These adsorption stoichiometries, without contributions from physisorption, and the color changes detected indicate that thiophene adsorption occurs concurrently with oligomerization on acidic OH groups and that oligomer size depends on spatial constraints within channels. Thiophene oligomers decompose at ~534 K during subsequent thermal treatment to form molecular thiophene with all carriers, leaving behind unsaturated thiophene-derived species with a 0.9–1.1 thiophene/Al stoichiometry, confirming the specificity of OH groups and the oligomeric nature of bound thiophene during adsorption at 363 K. With He, H<sub>2</sub>, and C<sub>3</sub>H<sub>8</sub>, residual thiophene-derived species desorb as stable fragments, such as H<sub>2</sub>S, ethene, propene, arenes, and heavier organosulfur compounds (methylthiophene and benzothiophene) during thermal treatment; they also form unsaturated organic deposits that cannot desorb without hydrogenation events. H<sub>2</sub> and C<sub>3</sub>H<sub>8</sub> remove larger amounts of adsorbed species as unreacted thiophene than He, suggesting that dehydrogenation reactions are inhibited or reversed by a hydrogen source. C<sub>3</sub>H<sub>8</sub> removes a larger fraction of thiophene-derived intermediates as hydrocarbons and organosulfur compounds than H<sub>2</sub> or He; thus, hydrogen atoms formed during C<sub>3</sub>H<sub>8</sub> dehydrogenation are more effective in the removal of unsaturated deposits than those formed from H<sub>2</sub>. Thiophene-derived adsorbed species are completely removed only with O<sub>2</sub>-containing streams at 873 K, a process that fully recovers initial adsorption capacities. This study provides a rigorous assessment of the nature and specificity of thiophene adsorption processes on acidic OH groups and of the identity and removal pathways of adsorbed species in various reactive environments.

## Introduction

Stringent effluent and fuel specifications for environmental protection have led to renewed interest in catalytic and adsorption processes for removing traces of organosulfur compounds from hydrocarbon streams.<sup>1,2</sup> Current hydrodesulfurization strategies (HDS) involve catalytic treatments with H<sub>2</sub> to remove organosulfur compounds as H<sub>2</sub>S, which is ultimately captured and converted to elemental sulfur. These processes require H<sub>2</sub>, often at high pressures, and tend to saturate high-octane alkene and arene components in fuels, resulting in undesirable loss of octane. As a result, hydrodesulfurization becomes less useful for gasoline than for diesel fuels, for which hydrogenation of unsaturated components can actually increase fuel quality.

We consider here adsorption processes for the selective removal of organosulfur compounds. Several recent studies have addressed their adsorptive removal using zeolites, carbon, or alumina porous solids. Weitkamp et al.<sup>3</sup> first

reported selective adsorption of thiophene in benzene mixtures using ZSM-5 zeolites. Adsorption from a gaseous stream containing 0.18 kPa thiophene led to 0.21 adsorbed thiophene molecules per framework Al atom at 323 K. King et al.<sup>4</sup> used H-ZSM5 to adsorb thiophene, methylthiophene, and dimethyl-thiophene from their gaseous mixtures with toluene or *p*-xylene and found that organosulfur molecules were selectively adsorbed relative to the more abundant arenes. Adsorption capacities were slightly lower (0.13 thiophene/Al at 363 K, 0.1 kPa of thiophene) than reported in ref 3, possibly because of the higher temperatures, lower thiophene pressures, and competitive adsorption with larger arenes.

Most practical adsorptive separations exploit van der Waals interactions between adsorbates and surfaces without chemical transformations of adsorbed species. King et al.<sup>4</sup> suggested that specific chemical interactions, and even chemical reactions leading to more strongly bound organosulfur compounds, account for the specificity of acid sites toward organosulfur compounds. Hernandez-Maldonado et al.<sup>5,6</sup> and Takahashi et al.<sup>7</sup> found that adsorbents based on Y-zeolites exchanged with Cu or Ag

\* Corresponding author. Tel: (510) 642-9673. Fax: (510) 642-4778. E-mail: iglesia@cchem.berkeley.edu.

<sup>†</sup> University of California at Berkeley.

<sup>‡</sup> ExxonMobil Research and Engineering.

(1) EPA Staff Paper on Gasoline Sulfur Issues, 1998, U.S. Environmental Protection Agency Office on Mobile Sources.

(2) Wormsbecher, R. F.; Weatherbee, G. D.; Kim, G.; Dougan, T. J. *National Petroleum Refiners Association Annual Meeting*, 1993, San Antonio.

(3) Weitkamp, J.; Schwark, M.; Ernst, S. *J. Chem. Soc., Chem. Commun.* **1991**, 1133.

(4) King, D. L.; Faz, C.; Flynn, T. *SAE 2000 World Congress*, Society of Automotive Engineers, Detroit, MI, March 6–9, 2000; Paper 2001-0002, pp 1–5.

(5) Hernandez-Maldonado, A. J.; Yang, R. T. *Ind. Eng. Chem. Res.* **2003**, *42*, 123–129.

(6) Hernandez-Maldonado, A. J.; Yang, R. T. *J. Am. Chem. Soc.* **2004**, *126*, 992–993.

(7) Takahashi, A.; Yang, F. H.; Yang, R. T. *Ind. Eng. Chem. Res.* **2002**, *41*, 2487–2496.

**Table 1. Physicochemical Properties of H-ZSM5 and H-Y Zeolites**

	H-ZSM5	H-ZSM5	HY-13	HY-85
crystal structure	Pentasil (MFI)	Pentasil (MFI)	Faujasite (FAU)	Faujasite (FAU)
channel size (Å)	5.3 × 5.6 5.1 × 5.5	5.3 × 5.6 5.1 × 5.5	7.4 × 7.4	7.4 × 7.4
particle size (nm)	200	250	300	400
Si/Al	13	40	13	85
Na (wt %)	0.02	0.03	0.01	0.003
Fe (wt %)	0.02	0.02	0.01	0.01
BET area (m <sup>2</sup> /g)	400	425		
pore volume (cm <sup>3</sup> /g)	0.128	0.129	0.326	0.301
Al <sub>framework</sub> /Al <sub>total</sub> <sup>a</sup>	0.91		0.92	0.84

<sup>a</sup> Framework Al/total Al ratio of calcined sample. Calculated from <sup>27</sup>Al NMR analysis.

cations selectively adsorbed thiophene in benzene via strong  $\pi$ -complexes, which decomposed upon evacuation at 623 K.<sup>8</sup> These studies reported saturation uptakes corresponding to thiophene/Cu(I) ratios above unity on Cu-Y zeolite, suggesting that processes other than  $\pi$ -complexation also bind thiophene. These pathways may involve specific thiophene interactions with protons, which form during exchange or reduction of Cu<sup>2+</sup> cations, nonspecific interactions and pore condensation, or oligomerization to form organosulfur molecules with much lower vapor pressures than thiophene. Thus, selective thiophene adsorption via  $\pi$ -complexation appears to occur in parallel with less selective adsorption and reaction processes.

The regeneration of saturated adsorbents has been examined less thoroughly than adsorption processes. The zeolitic adsorbents in previous studies were treated below 623 K in N<sub>2</sub>, a process that did not recover initial adsorption capacities.<sup>3–6</sup> Treatment in air above 623 K recovered fresh adsorption capacities by removing coadsorbed species, derived from arenes and alkenes in reactant mixtures, as CO<sub>2</sub> and H<sub>2</sub>O. Recently, Yu et al.<sup>9,10</sup> reported that sulfur removal from thiophenic compounds can be coupled kinetically with alkane dehydrogenation reactions to form H<sub>2</sub>S selectively, while incorporating the thiophenic carbons into useful hydrocarbons. Thus, we consider here the use of light alkanes for adsorbent regeneration and compare their effectiveness and selectivity to those of regeneration protocols using He, H<sub>2</sub>, and O<sub>2</sub>.

Several studies have addressed thiophene adsorption and decomposition pathways on zeolites.<sup>11–17</sup> Garcia et al.<sup>11,12</sup> used infrared spectroscopy and thermal desorption to probe thiophene adsorption and surface reactions on H-ZSM5, Na-ZSM5, and K-ZSM5, without concurrent determinations of reaction rates or selectivities. Yu et al.<sup>17</sup> examined adsorption and subsequent reactions of thio-

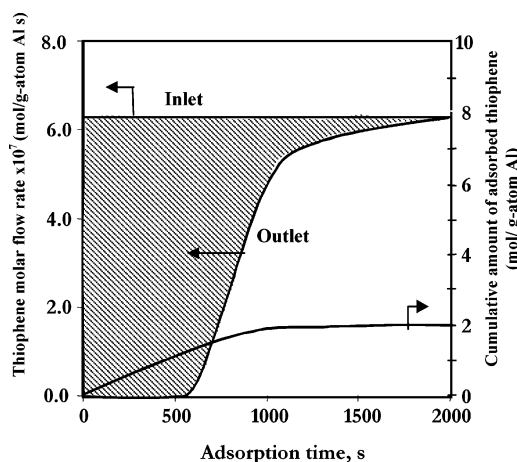


**Figure 1.** Thiophene molar flow rate and total accumulative amount of adsorbed thiophene per g-atom of Al on H-ZSM5 (Si/Al = 13) at 363 K versus adsorption time. The integrated area between the inlet and outlet curves represents the total amount of adsorbed thiophene.

phene during thermal treatment in He or H<sub>2</sub> on H-ZSM5 and Co/H-ZSM5 using infrared spectroscopy.

Here, we report rates and selectivities for reactions of adsorbed thiophene on H-ZSM5 using O<sub>2</sub>, He, H<sub>2</sub>, and C<sub>3</sub>H<sub>8</sub> streams. We also report thiophene adsorption stoichiometries and the identity and yield of products formed during thiophene adsorption and during subsequent desorption and reactions of thiophene-derived adsorbed species. These studies have led to a rigorous assessment of the type and location of thiophene-derived species and to specific suggestions about the mechanism for desorption and reaction of these adsorbed species in various reactive environments.

## Experimental Section

**Adsorbent Composition and Properties.** NH<sub>4</sub>-ZSM5 (AlSi-Penta, Si/Al = 13 (lot 97EB-6197)) was converted to the acid form by treatment at 773 K for 3 h in flowing dry air (Airgas, C.P. > 99.9%). H-ZSM5 (Si/Al = 40, CBV 5014 (lot 1822-80)) was obtained from Zeolyst Corp. in its acid form. H-Y samples (Si/Al = 13 (MC-5876, lot 18510-125-B) and Si/Al = 85 (MC-5878, lot 21074-126-B)) were prepared by dealumination of high-silica ECR-32<sup>18</sup> by H<sub>4</sub>EDTA and steaming/acid treatments. Using the method described in ref 18, a high silica FAU sample was prepared from a gel with 9.6 TPAOH/1.6 Na<sub>2</sub>O/Al<sub>2</sub>O<sub>3</sub>/24 SiO<sub>2</sub>/350 H<sub>2</sub>O/0.72 Na<sub>2</sub>SO<sub>4</sub> stoichiometry, where TPAOH is tetrapropylammonium hydroxide and 10% of the alumina came from a seed solution with a SiO<sub>2</sub>/Al<sub>2</sub>O<sub>3</sub> ratio of 17.5. The recovered product (Si/Al = 5.1) was treated in ambient air at 873 K for 3 h to remove the template. This treated ECR-32 (100 g) was placed in refluxing H<sub>2</sub>O (1500 g) for 20 h using a Soxhlet extractor, and H<sub>4</sub>EDTA (30.3 g) was added slowly.<sup>19</sup> The product was recovered by filtration and washed with distilled H<sub>2</sub>O. This dealuminated sample was converted to its ammonium form by four sequential exchanges with 10% NH<sub>4</sub>Br solutions at 333 K for 1 h. After the second and third exchanges, the sample was treated in ambient air at 623 K for 3 h. The Si/Al ratio was 13 by elemental analysis (ICP-AES) and is designated HY-13. Another portion of the initial air-treated ECR-32 was converted to its ammonium form by four sequential exchanges with 10% NH<sub>4</sub>Cl solutions at 333 K. After the second and fourth exchanges, the sample was treated in ambient air at 573 K for 3 h. This NH<sub>4</sub>FAU sample (175 g) was then treated with 100% steam at 950 K for 5 h and then with 2.63 L of 0.5 N HCl under reflux for 3 h. The product was recovered by filtration and washed with distilled H<sub>2</sub>O to give a sample with a Si/Al ratio of 85 (HY-85). The physicochemical properties of

(8) King, C. J. Separation Processes Based on Reversible Chemical Complexion. In *Handbook of Separation Process Technology*; Rousseau, R. W., Ed.; Wiley: New York, 1987; Chapter 15.

(9) Yu, S. Y.; Li, W.; Iglesia, E. *J. Catal.* **1999**, *187*, 257.

(10) Li, W.; Yu, S. Y.; Iglesia, E. *Stud. Surf. Sci. Catal.* **2000**, *130*, 899–904.

(11) Garcia, C. L.; Lecher, J. A. *J. Phys. Chem.* **1992**, *96*, 2669.

(12) Garcia, C. L.; Lecher, J. A. *J. Mol. Struct.* **1993**, *293*, 235.

(13) Geobaldo, F.; Palomino, G. T.; Bordiga, S.; Zecchina, Z.; Arean, C. O. *Phys. Chem. Chem. Phys.* **1999**, *1*, 561–569.

(14) Spoto, G.; Geobaldo, F.; Bordiga, S.; Lamberti, C.; Scarano, D.; Zecchina, A. *Top. Catal.* **1999**, *8*, 279–292.

(15) Mills, P.; Korlann, S.; Bussel, M.; Reynolds, M. A.; Ovchinnikov, M. V.; Angelici, R. J.; Sinner, C.; Weber, T.; Prins, R. *J. Phys. Chem. A* **2001**, *105*, 4418.

(16) Mills, P.; Phillips, D. C.; Woodruff, B. P.; Main, R.; Busell, M. E. *J. Phys. Chem. B* **2000**, *104*, 3237.

(17) Yu, S. Y.; Garcia-Martinez, J.; Li, W.; Meitzner, G. D.; Iglesia, E. *Phys. Chem. Chem. Phys.* **2002**, *4*, 1241–1251.

(18) Vaughan, D. E. W.; Strohmaier, K. G. U.S. Patent 5,549,881, 1996.

(19) Kerr, G. T. *J. Phys. Chem.* **1968**, *72*, 2594.

**Table 2. Comparison of Total Amount of Adsorbed Thiophene, Removed Thiophene during Flushing, Retained Thiophene after Flushing at 363 K, Desorbed Thiophene as Unreacted Thiophene, Desorbed Thiophene as Other Products, and Retained Thiophene after Regeneration of H-ZSM5 Zeolite (Si/Al = 13) Using He, H<sub>2</sub>, C<sub>3</sub>H<sub>8</sub>, or O<sub>2</sub> as Carrier Gases<sup>a</sup>**

total thiophene adsorbed (molecules/Al)	thiophene removed during flushing (molecules/Al)	thiophene retained after flushing (molecules/Al)	regeneration carrier gas	thiophene desorbed unreacted (molecules/Al)	thiophene desorbed as other products (molecules/Al)	thiophene retained after regeneration (molecules/Al)
Desorption $T = 773$ K						
2.05	0.3	1.75	He	0.59	0.11	1.05
2.01	0.35	1.66	H <sub>2</sub>	0.75	0.14	0.91
2.07	0.33	1.74	C <sub>3</sub> H <sub>8</sub>	0.7	0.17	0.87
2.03	0.28	1.67	O <sub>2</sub>	0.48	1.04	0.15
Desorption $T = 873$ K						
1.99	0.33	1.66	He	0.6	0.13	0.93
1.98	0.36	1.62	H <sub>2</sub>	0.67	0.16	0.79
2.01	0.3	1.71	C <sub>3</sub> H <sub>8</sub>	0.67		
2.08	0.23	1.85	O <sub>2</sub>	0.43	1.42	0

<sup>a</sup> Adsorption conditions: 363 K, 1 kPa thiophene, balance He. Desorption conditions: heating rate of 0.42 K s<sup>-1</sup> and final regeneration temperatures of 773 and 873 K.

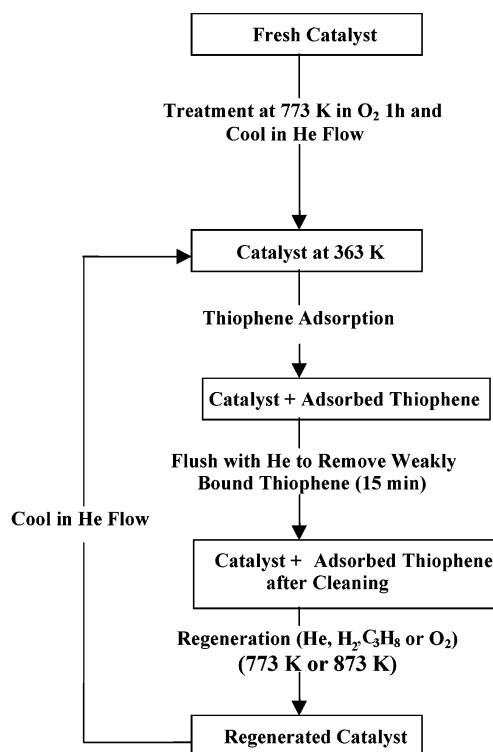
these samples are shown in Table 1. Each sample was pelleted and sieved into granules with 180–335  $\mu\text{m}$  diameter before adsorption–desorption measurements.

**Thiophene Adsorption–Desorption Experiments.** Zeolite adsorbents (0.25 g) were placed within a quartz cell and treated in flowing dry air (Airgas, C.P. >99.9%) at 773 K for 1 h. Adsorption measurements were carried out at 363 K using 0.4 cm<sup>3</sup> h<sup>-1</sup> liquid thiophene (Aldrich, >99%) introduced into a flowing He–Ar stream (Matheson, He/Ar (95/5), 3.3 cm<sup>3</sup> s<sup>-1</sup>) with a precision syringe pump (Cole Palmer 74900). Thiophene was vaporized immediately upon injection at 423 K and transferred into the reactor and the analytical system through heated lines kept at 423 K. Thiophene concentrations in the reactor effluent were measured by mass spectrometry (Leybold Inficon Inc. Transpector). The 2–185 amu mass range was scanned every ~6 s, and intensities at 58 and 84 amu were used to measure thiophene concentrations. Typically, thiophene was initially depleted from inlet streams for a period of time, after which its concentration increased and ultimately reached inlet levels, as each adsorbent reached saturation coverages (Figure 1). Adsorbed amounts were measured from a time integral of the differences between inlet and outlet concentrations; cumulative adsorbed amounts obtained by this method are shown in the right axis of Figure 1. After saturation, samples were treated in He (Airgas, >99.99%, 1.7 cm<sup>3</sup> s<sup>-1</sup>) at 363 K for 0.25 h to remove weakly adsorbed thiophene before starting regeneration protocols.

The removal of adsorbed species via desorption or reaction was examined using four gas streams [O<sub>2</sub> (Airgas, as He/O<sub>2</sub> mixture (80/20)), He (Airgas, >99.99%), H<sub>2</sub> (Airgas, >99.99%), and C<sub>3</sub>H<sub>8</sub> (Matheson, as C<sub>3</sub>H<sub>8</sub>/Ar/He mixture (20/5/75))], a temperature ramp of 0.42 K/s from 363 K, and two final temperatures (773 and 873 K) held for 1 h. The effluent stream was analyzed continuously during desorption–reaction protocols with on-line mass spectrometry, as described above, and with gas chromatography (Hewlett-Packard 6890; capillary HP-1 cross-linked methylsilicone column, 50 m  $\times$  0.32 mm, 1.05  $\mu\text{m}$  film; packed Hayesep-Q column, 80/100 mesh, 10'  $\times$  0.125") using flame ionization and thermal conductivity detection. These analytical methods were used to determine the identity and concentrations of thiophene reaction products. These protocols (described in Scheme 1) were used for all adsorption–desorption cycles; each cycle was started with a fresh zeolite sample.

**Catalytic C<sub>3</sub>H<sub>8</sub> Dehydrocyclodimerization.** C<sub>3</sub>H<sub>8</sub> dehydrocyclodimerization rate and selectivity measurements were carried out in a quartz flow microreactor. C<sub>3</sub>H<sub>8</sub> conversion and selectivities were measured at 773 K using C<sub>3</sub>H<sub>8</sub> (20 kPa) (Matheson, as C<sub>3</sub>H<sub>8</sub>/Ar/He mixture (20/5/75)) from chromatographic analysis of effluent streams (Hewlett-Packard 6890) using capillary (HP-1 cross-linked methylsilicone column, 50 m  $\times$  0.32 mm, 1.05  $\mu\text{m}$  film) and packed columns (Hayesep-Q column, 80/100 mesh, 10'  $\times$  0.125") using flame ionization and thermal conductivity detectors. C<sub>3</sub>H<sub>8</sub> conversions are reported as the percentage of C<sub>3</sub>H<sub>8</sub> fed that disappears during reaction. Product selectivities are reported on a carbon basis as the percentage of the converted C<sub>3</sub>H<sub>8</sub> that appears as each product.

**Scheme 1. Thiophene Adsorption–Desorption Cycles Carried out on H-ZSM5 Zeolite (Si/Al = 13)<sup>a</sup>**



<sup>a</sup> TPH, thiophene.

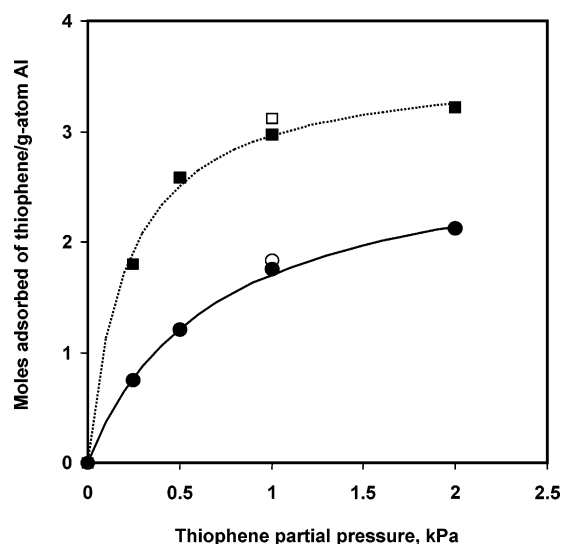
## Results and Discussion

**Adsorption of Thiophene on H-ZSM5 Zeolite.** A packed bed of each sample (0.25 g) was treated in air at 773 K for 1 h; it was then exposed to a (1% mol) thiophene/He stream, and outlet concentrations were measured continuously by mass spectrometry. The sample was then flushed with pure He [363 K; 1.7 cm<sup>3</sup> s<sup>-1</sup> He] for 0.25 h. Only thiophene was detected in the effluent (0.3 thiophene/Al) during this treatment, but most of the adsorbed thiophene was retained by the samples during treatment in He at 363 K. Thiophene uptakes were calculated from the difference between the amounts of thiophene initially removed from the inlet stream and evolved during subsequent treatment in He.

The thiophene adsorbed on H-ZSM5 (Si/Al = 13) after treatment in He at 363 K was ~1.7 thiophene/Al (Table 2), which exceeds adsorption uptakes previously reported

**Table 3. Thiophene Adsorption Capacities of H-ZSM5 Samples Reported by Different Authors Compared with the Thiophene Adsorption Capacities Obtained in This Work Using H-ZSM5 (Si/Al = 13 and 40) and H-Y (Si/Al = 13 and 85) Zeolites**

reference	zeolite	Si/Al	partial pressure of thiophene (kPa)	partial pressure of toluene or benzene (kPa)	adsorption temperature (K)	thiophene retained after flushing (molecules/Al)	toluene or benzene retained after flushing (molecules/Al)
Weitkamp et al. [3]	H-ZSM5	20	0.18	23.3 (benzene)	323	0.21	not reported
King et al. [4]	H-ZSM5	14.5	0.10	3.20 (toluene)	363	0.13	not reported
Yu et al. [17]	H-ZSM5	14.5	1		room temp	1.62	
this work	H-ZSM5	13	1		363	1.75	
this work	H-ZSM5	40	1		363	1.83	
this work	H-ZSM5	13	0.15	3.00 (toluene)	363	0.19	0.37 (toluene)
this work	HY-13	13	1		363	2.97	
this work	HY-85	85	1		363	3.12	

**Figure 2.** Adsorption isotherms for thiophene on H-ZSM5 (Si/Al = 13) and H-Y (Si/Al = 13) zeolites at 363 K. The points represent experimental data: (●) H-ZSM5 (Si/Al = 13), (○) H-ZSM5 (Si/Al = 40), (■) H-Y (Si/Al = 13), and (□) H-Y (Si/Al = 85). The lines represent the calculated isotherms using a Langmuir type equation (using the first component of eq 2): (—) H-ZSM5 (Si/Al = 13) and (···) H-Y (Si/Al = 13).

on H-ZSM5 (Table 3).<sup>3,4,17</sup> These lower previous values (Table 3) may reflect the lower thiophene concentrations in previous studies (0.10–0.20 kPa) compared with those used here (1 kPa), competitive adsorption by arene components in the thiophene-containing streams, or differences in structural purity for zeolite samples. We have probed the first two possibilities by measuring thiophene adsorption isotherms with and without toluene in the flowing stream.

A thiophene–toluene mixture (363 K, 0.15 kPa thiophene, 3.0 kPa toluene) was passed over H-ZSM5 (Si/Al = 13), and the adsorption of each component was measured from differences between inlet and outlet concentrations. The thiophene adsorption uptake after flushing for 0.25 h in He was 0.19 molecules per Al (Table 3), a value much lower than obtained at 0.15 kPa without toluene (0.56 thiophene/Al); this behavior is consistent with competitive adsorption of toluene and thiophene on zeolite adsorption sites. The thiophene adsorption selectivity relative to toluene is defined as

$$S_{\text{Th}} = [(X_{\text{Th}})/(P_{\text{Th}})]/[(X_{\text{Tol}})/(P_{\text{Tol}})] \quad (1)$$

where  $X_{\text{Th}}$  and  $X_{\text{Tol}}$  are the moles of thiophene and toluene adsorbed per Al, respectively, and  $P_{\text{Th}}$  and  $P_{\text{Tol}}$  are their respective partial pressures. Its value was 10.2 at 363 K, indicating modest adsorbent specificity for thiophene over toluene. This ratio is greater than expected from the vapor

**Table 4. Thiophene Adsorption Characteristics for H-ZSM5 (Si/Al = 13) and H-Y (Si/Al = 13) Zeolites at 363 K**

sample	Si/Al (mole)	$C_t$ (mol thiophene g-atom Al)	$K_A$ (kPa <sup>-1</sup> )	correlation factor ( $R^2$ )
H-ZSM5	13	2.86	1.47	0.998
HY-13	13	3.59	4.57	0.999

pressures for thiophene and toluene ( $P_{\text{VTh}}/P_{\text{VTol}} = 2.2$  at 363 K<sup>20,21</sup>), suggesting that adsorption specificity exceeds those expected from van der Waals interactions. This selectivity value indicates, however, that a large fraction of the adsorption sites in H-ZSM5 will be occupied by abundant toluene instead of minority organosulfur compounds during contact with practical hydrocarbon streams.

The high adsorption uptakes reported here and by Yu et al.<sup>17</sup> on H-ZSM5 zeolite (Si/Al = 14.5) with pure thiophene streams (~1.6 thiophene/Al, 303 K, 1 kPa) led us to consider the specificity of thiophene adsorption on zeolitic protons and the potential contributions of non-specific van der Waals interactions within zeolite channel walls. These processes were probed by measuring adsorption isotherms over a range of thiophene partial pressures (0.25–2 kPa) at 363 K (Figure 2) on H-ZSM5 (Si/Al = 13) and H-Y zeolite (HY-13, Si/Al = 13). Thiophene adsorption can occur by chemisorption of thiophene on acid sites or nonselective adsorption (physisorption) via interactions with channel walls. These concurrent processes can be described using Langmuirian and Henry's law descriptions generally used to describe adsorption on zeolites<sup>22–24</sup> (eq 2):

$$C_{\text{ads}} = \frac{C_t K_1 P_{\text{th}}}{1 + K_1 P_{\text{th}}} + \frac{K_2 P_{\text{th}}}{\text{chemisorption on acid sites}} + \frac{\text{physisorption on channel walls}}{\text{physisorption on channel walls}} \quad (2)$$

where  $K_1$  and  $K_2$  are thiophene adsorption constants,  $C_t$  is the total number of specific binding sites, and  $P_{\text{th}}$  is the thiophene partial pressure. Langmuirian adsorption on acid sites is represented by the first term in eq 2, while thiophene physisorption processes are described by the second term.

(20) Williamham, C. B.; Taylor, W. J.; Pignocco, J. M.; Rossini, F. D., Vapor Pressures and Boiling Points of Some Paraffin, Alkylcyclopentane, Alkylcyclohexane, and Alkylbenzene Hydrocarbons. *J. Res. Natl. Bur. Stand.* **1945**, *35*, 219–244.

(21) Waddington, G.; Knowlton, J. W.; Scott, D. W.; Oliver, G. D.; Todd, S. S.; Hubbard, W. N.; Smith, J. C.; Huffman, H. M. Thermodynamic properties of thiophene. *J. Am. Chem. Soc.* **1949**, *71*, 797–808.

(22) Drago, R. S.; Webster, C. E.; McGiluray, J. W. *J. Am. Chem. Soc.* **1998**, *120*, 538.

(23) Webster, C. E.; Cottone, A., III; Drago, R. S. *J. Am. Chem. Soc.* **1999**, *121*, 12127.

(24) Webster, C. E.; Cottone, A., III; Drago, R. S. *Microporous Mesoporous Mater.* **1999**, *33*, 291.

**Table 5.** C<sub>3</sub>H<sub>8</sub> Conversion and Carbon Selectivity Obtained during C<sub>3</sub>H<sub>8</sub> Dehydrocyclodimerization and Cracking Reaction on H-ZSM5 (Si/Al = 13)<sup>a</sup>

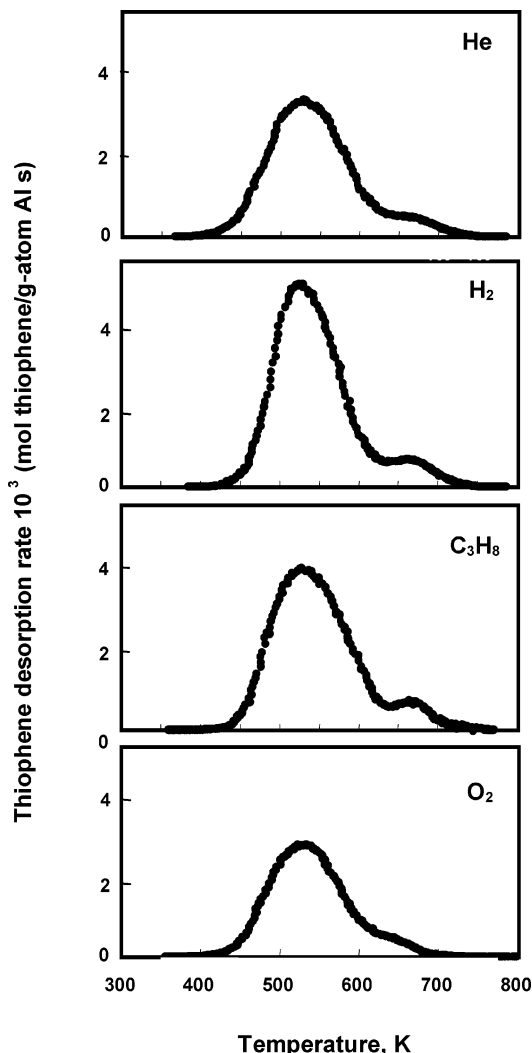
reaction T>bb	fresh catalyst			catalytic activity after regeneration treatment at 873 K			
	773 K	748 K	723 K	773 K with He	773 K with H <sub>2</sub>	773 K with C <sub>3</sub> H <sub>8</sub>	773 K with O <sub>2</sub>
conversion (% mol)	10.2	3.6	2.5	2.2	3.3	4.4	10.3
carbon selectivity, %C							
C1-C2	64.2	65.7	68.3	69.9	66.6	64.8	65.0
propene	20.3	24.2	24.7	26.1	24.1	22.1	19.7
C4	10.6	7.7	7.0	4.0	8.0	9.1	9.7
C6 + aromatic	4.9	2.4	0.0	0.0	1.3	3.8	5.6

<sup>a</sup> Results obtained using fresh and regenerated H-ZSM5 samples (regeneration was carried out at 873 K for 1 h in O<sub>2</sub>, He, H<sub>2</sub>, or C<sub>3</sub>H<sub>8</sub> after thiophene adsorption). Reaction conditions: 773 K, contact time of 20 g-cat h mol<sup>-1</sup> C<sub>3</sub>H<sub>8</sub> fed and total pressure of 1 atm.

Thiophene adsorption isotherms and parameters at 363 K are shown for H-ZSM5 and H-Y with similar Si/Al ratios in Figure 2 and Table 4, respectively. Isotherms were accurately described using only the first term in eq 2, consistent with the essential absence of physisorbed thiophene after flushing samples with He at 363 K. These findings suggest that a specific adsorption stoichiometry per Al site should be observed for samples with varying Si/Al ratios. H-ZSM5 (Si/Al = 13,40) and H-Y (Si/Al = 13, 85) zeolites with similar pore volume and crystallinity but varying Al content were used to test this hypothesis. Table 3 shows that the adsorption stoichiometry was similar on all samples but differed from the value of unity expected for specific interactions between one thiophene and one Brønsted acid site. The absence of nonspecific interactions for thiophene adsorption on H-ZSM5 and H-Y at 363 K, together with adsorption stoichiometries above unity, suggests that thiophene oligomers may form when thiophene-containing streams contact acid sites at 363 K.<sup>13,17</sup>

Thiophene is a five-carbon aromatic heterocycle with a proton affinity similar to that of benzene;<sup>25</sup> unlike benzene, thiophene undergoes electrophilic attack in acid solutions<sup>26,27</sup> to form trimers (e.g., [2,4-*d*-(2-thienyl)-thiolane] in H<sub>3</sub>PO<sub>4</sub><sup>28</sup> and larger oligomers on cation-exchanged Y,<sup>29</sup> mordenite,<sup>29</sup> and montmorillonite.<sup>30</sup> Infrared studies carried out by Yu et al.<sup>17</sup> showed that thiophene oligomerizes on acid sites slightly above ambient temperatures (373 K) but then depolymerizes at higher temperatures, allowing some molecular desorption of thiophene. Thus, it appears that chemical reactions of adsorbed protonated thiophene monomers with other thiophene molecules lead to the high chemisorption stoichiometries reported here and to an adsorption specificity that favors thiophene over arenes. This conclusion is consistent with color changes observed during thiophene adsorption, which are typical of thiophene oligomers. H-Y samples showed even higher adsorption stoichiometries than H-ZSM5, apparently because oligomer chain length depends on steric constraints imposed by zeolite channels;<sup>13</sup> thus, oligomers form larger chains within larger Y-zeolite channels and supercages than within smaller ZSM5 channels.

**Desorption of Thiophene Preadsorbed on H-ZSM5 Using O<sub>2</sub>, He, H<sub>2</sub>, and C<sub>3</sub>H<sub>8</sub> as Carrier Gases.** The molecular desorption of preadsorbed thiophene and the

**Figure 3.** Thiophene desorption rates during regeneration of H-ZSM5 (Si/Al = 13) using O<sub>2</sub>, He, H<sub>2</sub>, and C<sub>3</sub>H<sub>8</sub> as carrier gases [Si/Al = 13, 0.42 K s<sup>-1</sup>, isothermal at 773 K, 1 h].**Table 6.** Amount of Desorbed Thiophene as Unreacted Thiophene at 668 K in O<sub>2</sub>, He, H<sub>2</sub>, and C<sub>3</sub>H<sub>8</sub> on H-ZSM5 (Si/Al = 13)

carrier gas in desorption process	mol desorbed thiophene/g-atom Al
O <sub>2</sub>	0.007
He	0.010
H <sub>2</sub>	0.011
C <sub>3</sub> H <sub>8</sub>	0.013

evolution of its reaction products were examined as the sample temperature was increased using inert (He) or reactive (O<sub>2</sub>, H<sub>2</sub>, or C<sub>3</sub>H<sub>8</sub>) molecules in the contacting stream. After removing weakly bound thiophene by

(25) Szulejko, J. E.; McMahon, T. B. *J. Am. Chem. Soc.* **1993**, *115*, 7839.

(26) Curtis, R. F.; Jones, D. M.; Thomas, W. A. *J. Chem. Soc. (C)* **1971**, 234.

(27) Jackson, A. H. *Chemistry of Heterocyclic Compounds*; Taylor, E. C., Weissenberg, A., Eds.; Interscience, John Wiley & Sons: New York, 1987; Vol. 48, Part I, p 305.

(28) Saintigny, X.; van Santen, R. A.; Clemendot, S.; Hutschka, F. *J. Catal.* **2001**, *200*, 79.

(29) Enzel, P.; Bein, T. *J. Chem. Soc., Chem. Commun.* **1989**, 1326.

(30) Lorprayoon, V.; Condrate, R. A. S. *Appl. Spectrosc.* **1982**, *36*, 696.

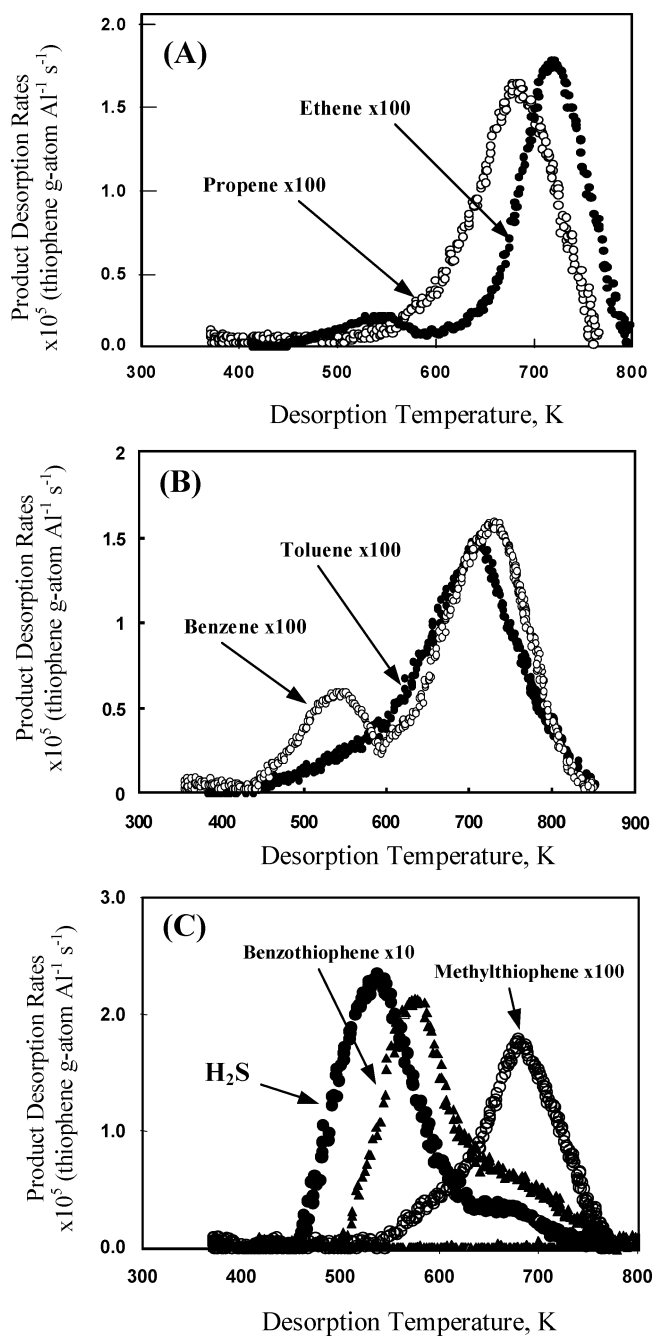


**Figure 4.** Desorption rates of the products obtained during regeneration of H-ZSM5 using H<sub>2</sub> as carrier [Si/Al = 13, 0.42 K s<sup>-1</sup>, isothermal at 773 K, 1 h]: (A) ethene and propene, (B) benzene and toluene, and (C) hydrogen sulfide, methylthiophene, and benzothiophene. The same desorption profiles were obtained when He and C<sub>3</sub>H<sub>8</sub> were used as carrier gases.

treating samples in He at 363 K for 0.25 h, the temperature was increased linearly (at 0.42 K s<sup>-1</sup>) to either 773 or 873 K and held for 1 h while the effluent stream was monitored continuously by mass spectrometry. He, H<sub>2</sub>, and C<sub>3</sub>H<sub>8</sub> did not restore initial adsorption capacities after treatment for 1 h at 773 or 873 K (Table 2), indicating that thiophene-derived chemisorbed species do not all desorb or react during these treatments. H<sub>2</sub> and C<sub>3</sub>H<sub>8</sub> removed a larger fraction of the initially adsorbed thiophene than He (Table 2), but neither treatment restored the initial white color of the zeolite samples. Treatment in O<sub>2</sub> (20 kPa) up to 873 K and holding at 873 K for 1 h restored initial adsorption uptakes and the white color of fresh samples, suggesting

**Table 7. Total Amount of Desorbed Products per g-atom of Al during Regeneration of H-ZSM5 with He, H<sub>2</sub>, C<sub>3</sub>H<sub>8</sub>, or O<sub>2</sub> as Carrier Gas [Si/Al = 13, 0.417 K s<sup>-1</sup>, Isothermal at 773 K, 1 h]<sup>a</sup>**

compound	O <sub>2</sub>	He	H <sub>2</sub>	C <sub>3</sub> H <sub>8</sub>
ethene	0.0 (719)	5.9 (721)	8.7 (720)	8.96 (716)
propene	0.4 (671)	3.7 (673)	6.1 (670)	10.25 (667)
benzene	0.3 (726)	5.8 (732)	9.3 (730)	11.7 (726)
toluene	0.3 (700)	4.9 (700)	6.4 (702)	13.8 (704)
thiophene	480.0 (531)	590.0 (535)	750.0 (544)	700.0 (534)
methylthiophene	0.1 (676)	3.2 (683)	5.7 (680)	8.2 (679)
benzothiophene	3.11 (569)	42.1 (572)	48.1 (568)	51.8 (568)
H <sub>2</sub> S	21.5 (532)	307.1 (531)	460.0 (531)	409.0 (530)
CO <sub>2</sub>	4100.0 (520)			
AC/OSC <sup>b</sup>	0.19	0.24	0.29	0.43

<sup>a</sup> Data in brackets represent the desorption temperature for each desorbed product (temperature in K). <sup>b</sup> AC, aromatic compounds (benzene + toluene); OSC, organosulfur compounds (methylthiophene + benzothiophene).

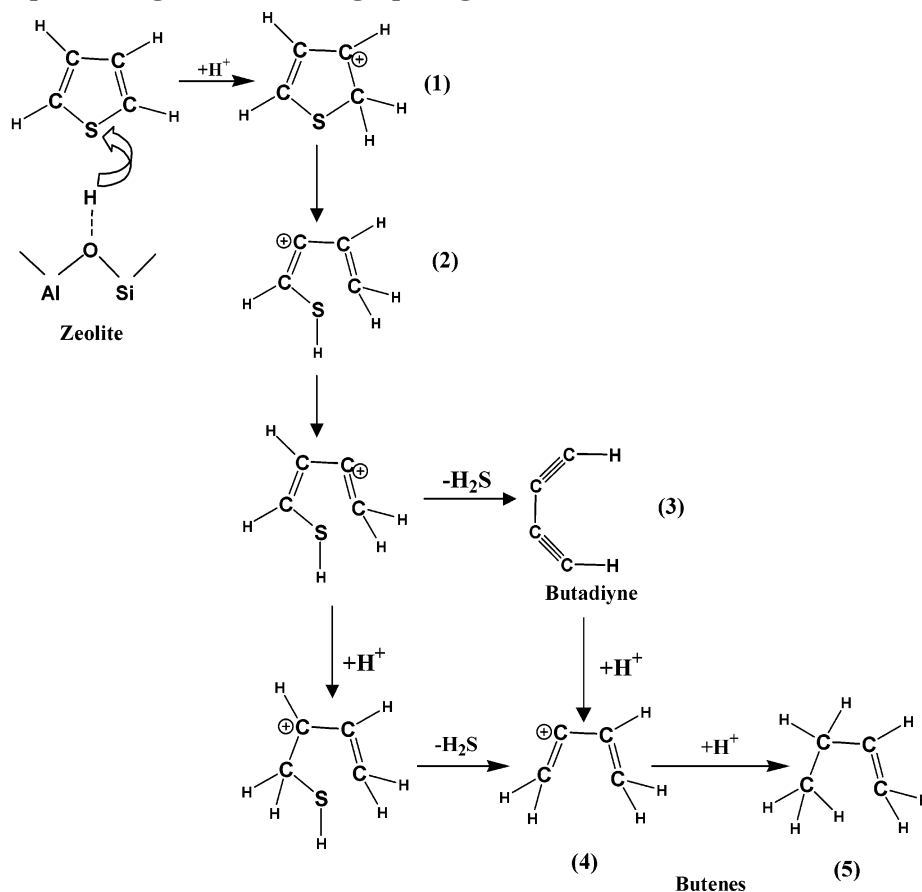
that these oxidative treatments removed all thiophene-derived residues.

Catalytic C<sub>3</sub>H<sub>8</sub> dehydrocyclodimerization and cracking rates were measured (at 773 K, 20 kPa C<sub>3</sub>H<sub>8</sub>) on H-ZSM5 (Si/Al = 13) before thiophene adsorption and after each regeneration protocol. The data in Table 5 show that only oxidative treatments at 873 K restored initial catalytic rates after thiophene adsorption. Treatments in He, H<sub>2</sub>, or C<sub>3</sub>H<sub>8</sub> (Table 5) did not restore initial catalytic rates but did recover initial selectivities, indicating that thiophene-derived residues merely titrate acid sites without significant modification of unblocked sites or of transport rate in H-ZSM5 channels. C<sub>3</sub>H<sub>8</sub> regeneration protocols led to higher propane dehydrocyclodimerization rates than procedures using He or H<sub>2</sub>, a finding consistent with the higher thiophene adsorption capacity measured after C<sub>3</sub>H<sub>8</sub> regeneration procedures.

Next, we describe the dynamics of product evolution during treatment of adsorbed thiophene with these carrier gases. Unreacted thiophene desorbed in two separate peaks (at 534 and 668 K) with O<sub>2</sub>, He, H<sub>2</sub>, or C<sub>3</sub>H<sub>8</sub> carriers. The shape and peak temperature of these two peaks were are similar for all carriers (Figure 3). The first desorption peak is larger than the second peak. Two desorption peaks for thiophene molecules were also observed on Na-ZSM5;<sup>11</sup> they were described as weakly adsorbed and strongly adsorbed thiophene molecules based on their desorption temperatures. Another study<sup>17</sup> attributed the low-temperature process to the desorption of physisorbed thiophene and the higher temperature process to specific interactions with cations (e.g., Na<sup>+</sup>, Fe<sup>3+</sup>, H<sup>+</sup>). The essential absence of physisorbed thiophene suggests that thiophene molecules desorb by depolymerization of thiophene oligomers in all carriers as temperature increases.

The amount of unreacted thiophene desorbed in the second peak (~0.1 thiophene/Al, Table 6) is similar to the combined amounts of Na and Fe in this H-ZSM5 sample (Na/Al = 0.008 and Fe/Al = 0.005); thus, this desorption peak may reflect interactions of thiophene with these cations. The total amount of thiophene that desorbs unreacted (Table 2) is greater with H<sub>2</sub> and C<sub>3</sub>H<sub>8</sub> than with He or O<sub>2</sub> as carrier gases. Thus, it appears that dehydrogenation reactions convert adsorbed thiophene to unreactive residues during thermal treatments carried out with the intent to desorb adsorbed thiophene. H<sub>2</sub> and C<sub>3</sub>H<sub>8</sub> appear to inhibit or reverse such reactions by providing hydrogen atoms required to prevent or reverse dehydrogenation reactions of adsorbed thiophene-derived intermediates.

The residual amounts of thiophene-derived species after molecular desorption at ~773 K correspond to adsorption

**Scheme 2. Thiophene Ring Activation, Ring-Opening Reaction, and Formation of H<sub>2</sub>S and C<sub>4</sub> Fragments**

stoichiometries near unity in all samples (0.9–1.1 thiophene/Al), irrespective of zeolite structure or Si/Al ratio (Table 2). These data indicate that these residual species correspond to specific irreversible interactions between thiophene and acidic OH groups. These irreversibly and clearly unsaturated residues desorb only via hydrogenation using sacrificial coadsorbed species (in He) or external H-sources (H<sub>2</sub>, C<sub>3</sub>H<sub>8</sub>) or via combustion pathways (in O<sub>2</sub>).

Thermal treatments in He, H<sub>2</sub>, or C<sub>3</sub>H<sub>8</sub> led to the formation of H<sub>2</sub>S, ethene, propene, benzene, toluene, methylthiophene, and benzothiophene as the predominant products. Desorption profiles and the nature of the products evolved were similar with He, H<sub>2</sub>, and C<sub>3</sub>H<sub>8</sub> (Figure 4a–c), but their relative amounts differed significantly among these carriers (Table 7). H<sub>2</sub>S forms at 534 K in He, H<sub>2</sub>, and C<sub>3</sub>H<sub>8</sub> (Figure 4a–c), apparently via ring-opening on thiophene-derived species to form unsaturated fragments, a reaction that occurs on Brønsted acid sites<sup>11,30–34</sup> via C–S bond cleavage of carbenium ion intermediates (Scheme 2, 1). This process forms H<sub>2</sub>S and adsorbed butadiyne species (Scheme 2, 3). On H-ZSM5, desulfurized thiophene fragments are highly unsaturated and unable to desorb as stable molecules without a separate source of hydrogen. Hydrogen transfer must occur for butadiynes (Scheme 2, 3) or ring-opened thiophenes (Scheme 2, 2) to form desorbable species (Scheme 2, 4 and 5). Hydrogen can be provided through adsorbed species

formed from C<sub>3</sub>H<sub>8</sub> or H<sub>2</sub> or via sacrificial hydrogen transfer from coadsorbed butadiyne species.

Benzene, toluene, methylthiophene, benzothiophene, and light hydrocarbons (ethene and propene) desorb at higher temperatures than H<sub>2</sub>S (Figure 4a–c). Thus, it appears that desulfurization occurs at low temperatures (~530 K) with the concurrent formation of unsaturated organic deposits. These deposits then react with other thiophene molecules as they desorb or with stranded thiophene-derived intermediates to form aromatics and larger organosulfur compounds. Stranded unsaturated deposits can also act as a stoichiometric source of hydrogen for hydrogenation, allowing the desorption of thiophene-derived species, especially when He is used as the carrier gas.

Benzene evolution occurs immediately upon heating preadsorbed thiophene above ambient temperatures, suggesting that it forms via hydrogenation of thiophene fragments remaining after ring opening and H<sub>2</sub>S evolution. The desorption temperatures and number of evolved benzene molecules resemble those for ethene (Figure 5), suggesting that they form via similar steps as depicted in Scheme 3. Species formed via thiophene desulfurization and condensation (Scheme 3, 6) can undergo subsequent ring opening and desulfurization to form product 7 (Scheme 3). Subsequent hydrogen transfer, cyclization, and cracking form benzene and ethene. Also, adsorbed butadiyne fragments can recombine with one another or with other thiophene-derived species to form ethene and aromatics after hydrogen transfer, cyclization, and cracking of ethyl side chains.

Propene and methylthiophene evolution profiles are also very similar in shape and intensity (Figure 6), suggesting a mechanistic connection between them. In Scheme 4,

(31) Saintigny, X.; van Santen, R. A.; Clemendot, S.; Hustchka, F. *J. Catal.* **1999**, *183*, 107.

(32) Luo, G. H.; Wang, X. Q.; Wang, X. S. *Chin. J. Catal.* **1998**, *19* (1), 53.

(33) Shan, H. H.; Li, C. Y.; Yang, C. H.; Zhao, H.; Zhao, B. Y.; Zhang, J. F. *Catal. Today* **2002**, *77*, 117–126.

(34) Corma, A.; Martinez, C.; Ketley, G.; Blair, G. *App. Catal.*, **A** **2001**, *208*, 135–152.

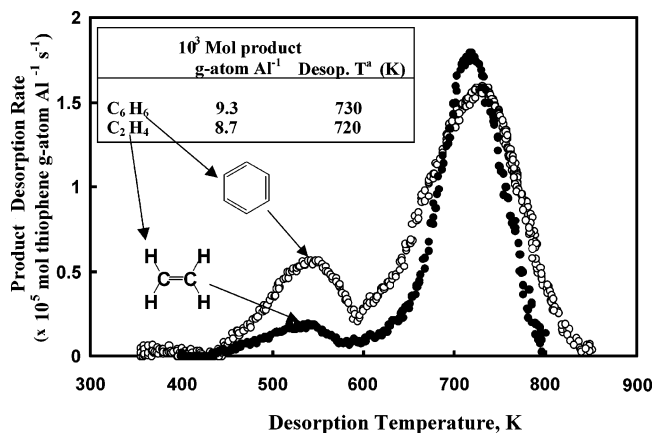
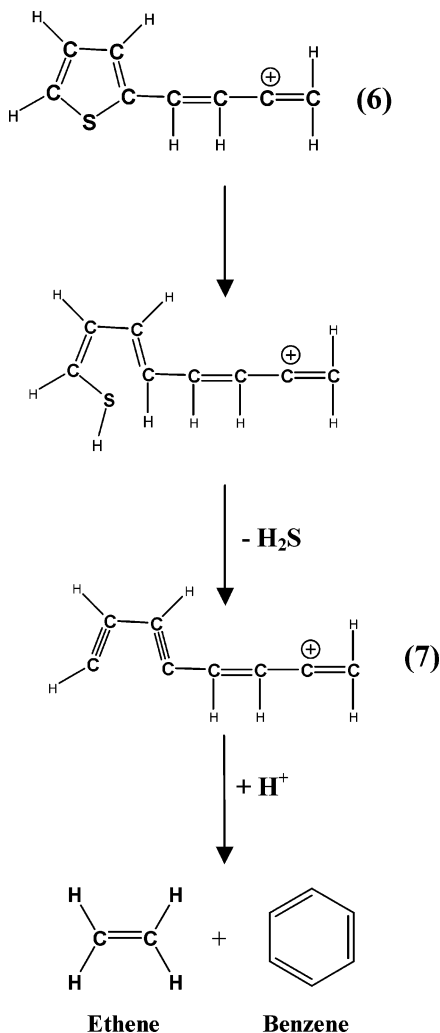


**Figure 5.** Benzene and ethene desorption rates, total desorption amounts, and desorption temperatures during regeneration of H-ZSM5 using H<sub>2</sub> as carrier [Si/Al = 13, 0.42 K s<sup>-1</sup>, isothermal at 773 K, 1 h].

### Scheme 3. Benzene and Ethene Formation Pathway



ring-opened thiophene-derived intermediates react with thiophene molecules to form products 8 or 9. After isomerization and hydrogen transfer, the C–S bond at the  $\beta$ -position cleaves to form H<sub>2</sub>S and butyl-thiophene (Scheme 4, 6 or 10). Butyl-thiophene can then react to form methylthiophene and propene after hydrogen transfer. Methylthiophene and propene can also form via reactions of adsorbed butadiyne with thiophene or

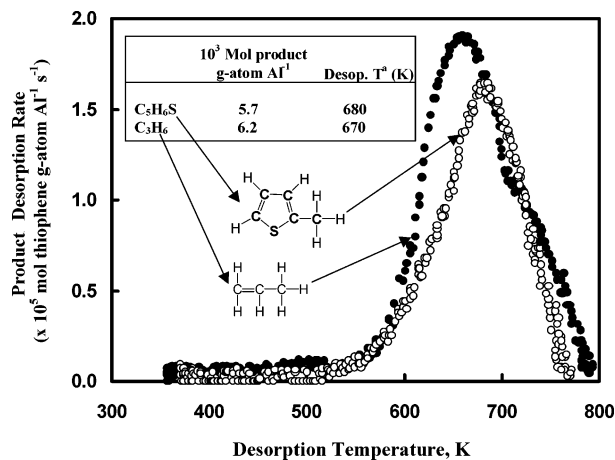


**Figure 6.** Methylthiophene and propene desorption rates, total desorption amounts, and desorption temperatures during regeneration of H-ZSM5 using H<sub>2</sub> as carrier [Si/Al = 13, 0.42 K s<sup>-1</sup>, isothermal at 773 K, 1 h].

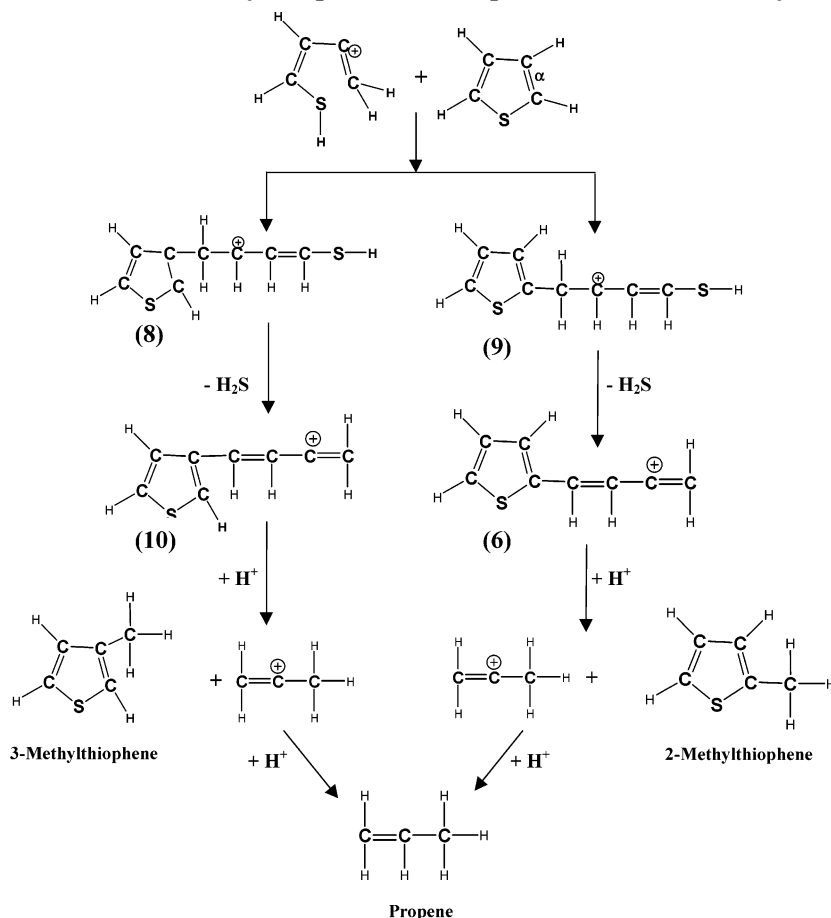
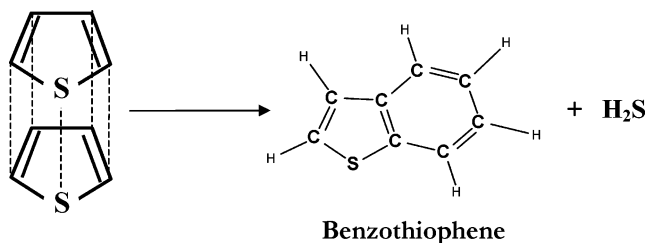
thiophene-derived intermediates followed by hydrogen transfer.<sup>33,34</sup>

Benzothiophene formed from preadsorbed thiophene during treatment with He, H<sub>2</sub>, and C<sub>3</sub>H<sub>8</sub> (Table 7) and desorbed in significant amounts at temperatures slightly higher than H<sub>2</sub>S (Figure 4c). This lower desorption temperature of benzothiophene (562 K) suggests that it forms as thiophene molecules desorb intact and react with bound thiophene in downstream sections of the adsorbent bed via Diels–Alder condensation reactions, which form H<sub>2</sub>S and benzothiophene (Scheme 5).<sup>9,10,35</sup> Benzothiophene can also form via cyclization of adsorbed butenylthiophenes (Scheme 6, 11).<sup>33</sup>

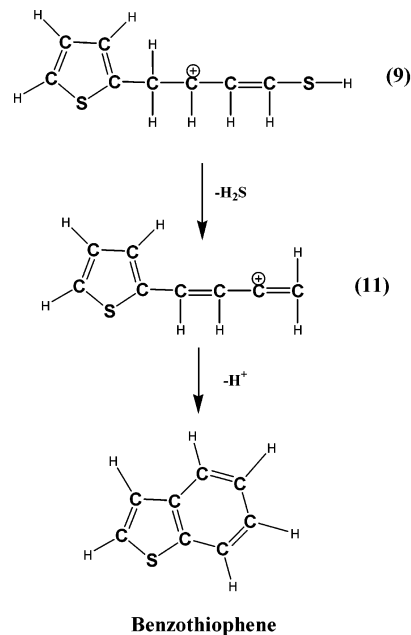
These proposed reactions, for which we provide quantitative experimental support here, are consistent with simulations of thiophene decomposition on Brønsted acid sites, which were shown to form H<sub>2</sub>S and adsorbed butadiyne fragments in the absence of an external hydrogen source.<sup>31</sup> Butadiyne adsorbs strongly and desorbs only after reactions with thiophene to form benzothiophene or with sacrificial hydrogen from coadsorbed unsaturated fragments. Adsorbed hydrogen or hydrogen-rich intermediates, available via alkane or H<sub>2</sub> dissociation, provide hydrogen without stoichiometric formation of stranded unsaturated residues.

The effectiveness of C<sub>3</sub>H<sub>8</sub> or H<sub>2</sub> in providing hydrogen-rich reagents for desorption of thiophene-derived fragments as stable molecules is illustrated in Table 7, which shows the amounts of products evolved during reactive desorption of adsorbed thiophene using H<sub>2</sub> or C<sub>3</sub>H<sub>8</sub> as carriers. C<sub>3</sub>H<sub>8</sub> led to the formation of ethene, propene, toluene, and benzene in concurrent catalytic dehydrocyclodimerization reactions. Thus, the products formed specifically from thiophene are difficult to distinguish from those formed in these catalytic reactions. In an attempt to circumvent this difficulty, we first treated fresh H-ZSM5 (Si/Al = 13) using the C<sub>3</sub>H<sub>8</sub> regeneration protocol, but without first adsorbing thiophene, and ethene, propene, toluene, and benzene formation rates were measured as a function of temperature. The differences between these formation rates and those measured during a similar treatment after thiophene adsorption were used to estimate the amounts of these products arising from reactions of C<sub>3</sub>H<sub>8</sub> with thiophene-derived species. The samples contain fewer remaining acid sites after thiophene adsorption; thus, C<sub>3</sub>H<sub>8</sub> dehydrocyclodimerization rates are



**Scheme 4. Methylthiophene and Propene Formation Pathway****Scheme 5. Benzothiophene Formation Pathway via Diels–Alder Reaction**

lower than on fresh samples subjected to the same regeneration protocol and the thiophene-derived amounts of ethene, propene, toluene, and benzene calculated in this way will be underestimated (Table 7). Nonetheless, these values provide useful measures of the role of  $C_3H_8$  during removal of thiophene-derived species from acid sites in H-ZSM5. Table 7 shows that larger amounts of arenes are formed from thiophene-derived species with  $C_3H_8$  than with  $H_2$ , apparently because alkenes and hydrogen species formed from propane convert butadiyne species to aromatics more effectively than hydrogen species formed via  $H_2$  dissociation. The ratio of arenes (benzene + toluene) to organosulfur (methylthiophene + dimethylthiophene + benzothiophene) products formed is greater with  $C_3H_8$  than with He or  $H_2$  as carriers. These results suggest that benzothiophene and methylthiophene formation is inhibited by scavenging of thiophene-derived intermediates to form desorbable species before bimolecular reactions of organosulfur species can occur, as also found during catalytic reactions of thiophene with  $H_2$  or light alkanes.<sup>9,35</sup>

**Scheme 6. Benzothiophene Formation Pathway via Alkylation–Cracking Reaction**

Regeneration in  $O_2$ -containing streams leads to the predominant formation of  $H_2O$ ,  $CO_2$ , and  $SO_2$  together with traces of unreacted thiophene, aromatics, and larger organosulfur compounds. The formation of  $CO_2$  and  $SO_2$  starts at temperatures slightly lower (520 K) than the desorption of unreacted thiophene and thiophene-derived organic molecules. These data suggest that these compounds can undergo oxidation reactions before desorption,

although some thiophene-derived species can desorb and undergo hydrogen transfer and Diels–Alder reactions before combustion, perhaps forming in the process more easily oxidized adsorbed organic residues. Regeneration with O<sub>2</sub>-containing streams is the only treatment that restored initial adsorption uptakes on H-ZSM5 (Table 2), but it leads to yield losses by forming undesired CO<sub>2</sub> and SO<sub>2</sub> products. Regeneration with alkanes allows the recovery of thiophene-derived carbon atoms into useful hydrocarbons but leads to incomplete regeneration of zeolite adsorbents and ultimately requires an oxidative treatment, which leads, however, to lower amounts of CO<sub>2</sub> and SO<sub>2</sub> because of the partial removal of organic residues during C<sub>3</sub>H<sub>8</sub> regeneration protocols.

### Conclusions

Thiophene adsorption–desorption on H-ZSM5 and H-Y zeolites has been studied. Thiophene adsorption uptakes were 1.7 and 2.8 thiophene/Al for H-ZSM5 (Si/Al = 13) and H-Y (Si/Al = 13), respectively. Similar adsorption uptakes were found for H-ZSM5 and H-Y samples with different Si/Al ratios (Si/Al = 13–85), indicating that these stoichiometries do not depend on zeolite Al content. Thiophene adsorption was also studied using thiophene–toluene mixtures. Thiophene selectivity ( $\sim 10$ ) was higher than expected from only van der Waals interactions. The adsorption stoichiometries, without physisorption contributions, and the color changes observed during thiophene adsorption suggest that thiophene oligomerization occurs on acid sites. H-Y zeolite showed higher adsorption uptakes than H-ZSM5, indicating that oligomer chain length depends on steric constraints imposed by zeolite channels. Thiophene oligomers decompose during thermal treatment forming molecular thiophene and leaving behind unsaturated thiophene-derived species with 1:1 (thiophene/Al) stoichiometry. These values confirm the specificity of OH groups and the oligomeric nature of bound thiophene formed during adsorption at 363 K.

Desorption experiments using O<sub>2</sub>, He, H<sub>2</sub>, and C<sub>3</sub>H<sub>8</sub> as carrier gases were also performed. Identification of reaction products suggests that the desorption–reaction pathways are similar when He, H<sub>2</sub>, or C<sub>3</sub>H<sub>8</sub> are used as carrier gases. The amounts of desorbed products, however, depend on the carrier gas. Regeneration under He removes less thiophene than under H<sub>2</sub> or C<sub>3</sub>H<sub>8</sub>, suggesting that the reactions that form unreactive species are dehydrogenation reactions. These dehydrogenation reactions generate species that can be hydrogenated to form desorbable hydrocarbons and H<sub>2</sub>S when hydrogen is available. H<sub>2</sub> and C<sub>3</sub>H<sub>8</sub> carriers have similar qualitative effects on thiophene desorption. Both H<sub>2</sub> and C<sub>3</sub>H<sub>8</sub> increased the amount of desorbed thiophene derivatives by providing a source of hydrogen. However, hydrogen atoms or gas-phase alkenes formed during propane dehydrogenation reactions on H-ZSM5 are more effective at removing the unsaturated hydrocarbons formed during thiophene desorption–reaction steps. Regeneration with O<sub>2</sub>-containing streams was the only treatment that restored initial adsorption uptakes on H-ZSM5; however, regeneration with alkanes allowed the recovery of thiophene-derived carbon atoms into useful hydrocarbons. In addition, oxidation treatment of zeolite adsorbents after regeneration with alkanes led to lower amounts of CO<sub>2</sub> and SO<sub>2</sub> because of the partial removal of organic residues during C<sub>3</sub>H<sub>8</sub> regeneration protocols.

**Acknowledgment.** Antonio Chica Lara gratefully acknowledges the Ministerio de Educacion, Cultura y Deportes de España and the Council for International Exchange of Scholars (CIES) for a Fulbright postdoctoral fellowship.

LA048320+